Clim. Past Discuss., 9, 3615–3662, 2013
www.clim-past-discuss.net/9/3615/2013/
doi:10.5194/cpd-9-3615-2013

Climate of the Past
Discussions
Open Access

The initiation of Neoproterozoic "snowball" climates in CCSM3: the influence of paleo-continental configuration

Y. Liu[1,*], **W. R. Peltier**[1], **J. Yang**[2,**], **and G. Vettoretti**[1]

[1]Department of Physics, University of Toronto, 60 St. George Street, Toronto, ON, M5S 1A7, Canada
[2]Dept. of Atmospheric and Oceanic Sciences, School of Physics, Peking University, Beijing, China
[*]now at: Woodrow Wilson School of Public and International Affairs, 410a Robertson Hall, Princeton University, Princeton, NJ, 08544, USA
[**]now at: The Department of the Geophysical Sciences, The University of Chicago, 5734 South Ellis Avenue, Chicago, IL 60637, USA

Received: 27 May 2013 – Accepted: 3 June 2013 – Published: 2 July 2013

Correspondence to: Y. Liu (yonggang@princeton.edu)

Published by Copernicus Publications on behalf of the European Geosciences Union.

Abstract

We identify the "hard snowball" bifurcation point at which total sea ice cover of the oceans is expected by employing the comprehensive coupled climate model CCSM3 for two realistic Neoproterozoic continental configurations, namely a low-latitude configuration appropriate for the 720 Ma Sturtian glaciation and a higher southern latitude configuration more appropriate for the later 635 Ma Marinoan glaciation. We find that for the same total solar insolation (TSI) and atmospheric CO_2 concentration (pCO_2), the most recent continental configuration is characterized by colder climate than the 720 Ma continental configuration and enters the hard snowball state more easily on account of the following four factors: the low heat capacity of land in the south polar region, the higher albedo of the snow covered land compared to that of sea ice, the more negative net cloud forcing near the ice front in the Northern Hemisphere (NH), and more importantly, the more efficient sea ice transport towards the equator in the NH due to the absence of blockage by continents. Beside the paleogeography, we also find the optical depth of aerosol to have a significant influence on this important bifurcation point. When the high value (recommended by CCSM3 but demonstrated to be a significant overestimate) is employed, the critical values of pCO_2, beyond which a hard snowball will be realized, are between 80–90 ppmv and 140–150 ppmv for the Sturtian and Marinoan continental configurations, respectively. However, if a lower value is employed that enables the model to approximately reproduce the present-day climate, then the critical values of pCO_2 become 50–60 ppmv and 100–110 ppmv for the two continental configurations, respectively. All of these values are higher than previously obtained for the present-day geography (17–35 ppmv) using the same model, primarily due to the absence of vegetation, but are much lower than that obtained previously for the 635 Ma continental configuration using the ECHAM5/MPI-OM model in its standard configuration (∼ 500 ppmv). However, when the sea ice albedo in that model was reduced from 0.75 to a more appropriate value of 0.45, the critical pCO_2 becomes ∼ 204 ppmv, closer to but still higher than the values obtained here. Our results are sim-

ilar to those obtained with the present-day geography (70–100 ppmv) when the most recent version of the NCAR model, CCSM4, is employed.

1 Introduction

Three distinct climate states have been proposed to be consistent with the global continental glaciations known to have occurred during the Neoproterozoic (1000–540 Ma), which themselves were inferred to have occurred on the basis of the low-latitude glaciogenic deposits that have been discovered over all major continents (e.g. Hoffman and Li, 2009). These states may be classified as either "hard" snowball (e.g. Kirschvink, 1992; Hoffman et al., 1998), "soft" snowball or slushball (e.g. Hyde et al., 2000; Peltier et al., 2004, 2007), or "thin-ice" snowball (e.g.Pollard and Kasting, 2005; Tziperman et al., 2012), respectively. In the hard snowball hypothesis, thick sea ice is assumed to have covered the entire surface of the oceans simultaneously with the continents being covered by thick ice-sheets during the glaciation events ("Sturtian" at ~ 720 Ma, "Marinoan" at ~ 635 Ma and perhaps also the "Gaskiers" glaciation at ~ 580 Ma), while in the soft snowball/slushball hypothesis, open ocean remains in the low latitude equatorial region so that both hydrological and photosynthetic processes would have remained active during such episodes of glaciation. The thin-ice snowball hypothesis, as is suggested by its name, argues that thin (sea) ice might have prevailed over the low latitude oceans, perhaps especially within marginal seas or isolated lakes during the glaciation events so that photosynthetic processes could persist, while the other parts of the planet were hard-snowball-like. In this sense, the thin-ice snowball is not a distinctly different climate state from the hard snowball, but in terms of biological activity it is identical to the "slushball" state. The fact that both photosynthetic and hydrological activity are strongly suspected to have continued throughout the Neoproterozoic interval has provided strong stimulus for the continuing effort to develop an alternative explanation to the hard snowball hypothesis for these deep glaciation events (Runnegar, 2000; Corsetti et al., 2006; Allen and Etienne, 2008).

CPD
9, 3615–3662, 2013

Since the geological and geochemical evidence is not sufficient to determine the sea ice state during any of the Neoproterozoic glaciations, the three hypotheses have been supported primarily on the basis of the different climate models employed by the different groups of proponents of the respective hypotheses. For example, Kirschvink (1992) proposed and Hoffman et al. (1998) have supported the hard snowball hypothesis based on the suggestion that the end state would have been governed by the action of runaway albedo feedback that obtains in the energy balance models (EBMs) of Budyko (1969) and Sellers (1969), which suggest that the Earth would rapidly enter a hard snowball state once the sea ice edge entends below $\sim 30^{\circ}$ latitude. However, later analyses based upon the use of the continent and ocean surface area resolving EBM of North et al. (1983) coupled to the continental ice-sheet model of Deblonde and Peltier (1990, 1991) demonstrated that the dynamical action of the continental ice-sheets supported the existence of steady-state slushball solutions (Hyde et al., 2000; Crowley et al., 2001) as did models which coupled the influence of the continental ice-sheets to an atmospheric general circulation model (AGCM) coupled in turn to a mixed-layer ocean model (Hyde et al., 2000). Subsequently, Pollard and Kasting (2005), and Tziperman et al. (2012) have suggested, using an alternative sea ice model (embodying the idea of sea-glaciers), that even in an overall hard snowball state, thin ice could exist in some isolated regions. How stable such thin ice might be in such isolated regions is clearly a concern.

In order to settle the debate between these three competing hypotheses, from a physical point of view, a model simulation which properly considers all of the relevant physical processes in the atmosphere, ocean, sea ice and land ice is required. The ideal model on the basis of which one might seek support for the soft snowball hypothesis, for example, would be an atmosphere–ocean general circulation model (AOGCM) coupled with an active land ice-sheet model, if this were able to adequately describe the initiation and development of global continental ice cover without leading to the ocean becoming completely ice covered. Unfortunately, such a model is still unavailable although both sophisticated AOGCM and land ice sheet models do clearly

CPD
9, 3615–3662, 2013

exist. Nevertheless the very long timescale over which such a coupled structure would have to be integrated ($\sim$ 100 kyr) associated with the formation of a snowball Earth (Donnadieu et al., 2003; Liu and Peltier, 2010, 2011) is not possible to contemplate on account of the computational resources that would be required. To adequately test the thin-sea ice hypothesis, a sea-glacier model such as that developed in Tzipperman et al. (2012) may be required to replace the sea ice module in the current AOGCMs as well as coupling to an explicit model of land ice-sheet evolution.

In the current state of research in this area, we are still several steps away from being able to reach the goal described above. Rather than applying a fully land-ice coupled AOGCM, only stand-alone AOGCMs have been applied (Poulsen et al., 2001, 2002; Donnadieu et al., 2004; Peltier et al., 2004; Poulsen and Jacob, 2004; Voigt and Marotzke, 2010; Voigt et al., 2011; Yang et al., 2012a, b, c) to search for the bifurcation point (in the space of, e.g., sea ice fraction versus radiative forcing, Voigt and Abbot, 2012), beyond which a hard snowball Earth, characterized solely in terms of total coverage of the oceans by sea ice, forms. Such models clearly cannot really be employed as a tool to argue definitively for or against the soft snowball hypothesis since a land ice sheet does not develop. For specific continental configurations, however, such models may be used to argue whether it is possible for an ice sheet to develop before entering a hard snowball state by considering the occurrence of perennial snow cover over the continents (Voigt et al., 2011). Such models do nevertheless represent an improvement over the AGCMs previously employed (e.g. Jenkins and Frakes, 1998; Jenkins and Smith, 1999; Chandler and Sohl, 2000) since they fully incorporate the influence of ocean dynamics.

The first relatively systematic study of the hard snowball bifurcation point using a reasonably modern AOGCM appears to have been that by Poulsen et al. (2001, 2002). The later resumption of such study using a more sophisticated AOGCM begin with the work of Voigt and Marotzke (2010) who employed the present-day continental configuration as basis for their analysis. Their results suggested that the Earth would enter a hard snowball state if the total solar irradiance (TSI) were reduced to somewhere between

CPD
9, 3615–3662, 2013

91–94 % of the present-day value (TSI_0, which is 1367 W m^{-2}) and greenhouse gas concentrations were kept the same as their pre-industrial values. The model they employed was the ECHAM5/MPI-OM, and with this particular model, no near-snowball "slushball" state was found to be stable, i.e. once sea ice cover exceeded ~ 57 % of the total ocean area, the climate quickly entered the hard snowball regime. However, with the same model, but for their more realistic Neoproterozoic continental configuration, Voigt et al. (2011) found that the Earth would enter a hard snowball state when TSI is reduced to between $0.955TSI_0$ and $0.96TSI_0$, or if the TSI is fixed at $0.94TSI_0$ (which is appropriate for the late Neoproterozoic, Gough, 1981), and the critical value of the atmospheric CO_2 concentration was between 500 and 556 ppmv, i.e. well above the modern level (see Voigt and Abbot, 2012). Again, no stable state was found in which the sea ice front could enter within 25° of the equator and the system remain stable in a "slushball" state.

By employing a different coupled AOGCM, namely the NCAR CCSM3, Yang et al. (2012a,b) demonstrated that for the present-day continental configuration, the critical values for both TSI and atmospheric CO_2 concentration (pCO_2) were much lower than those obtained using the ECHAM5/MPI-OM model, i.e. that it was much more difficult to form a hard snowball using this model. In particular it was found that the Earth would enter a hard snowball state only if the TSI were reduced to between $0.895TSI_0$ and $0.90TSI_0$ when pCO_2 is fixed to the pre-industrial value, or when pCO_2 is reduced to between 17.5 and 20 ppmv when TSI is fixed to $0.94TSI_0$. As important, however, concerning their results is the fact that this model delivered stable slushball solutions in which the sea ice front lay considerably equatorward of 25–30° latitude. When a more advanced version of the model, CCSM4, was employed, these critical values at the bifurcation point were found to increase moderately to 0.91–$0.92TSI_0$ and 70–100 ppmv, respectively (Yang et al., 2012c). Therefore, the conditions required for the initiation of a hard snowball Earth have been found to be highly model dependent, the transition being much easier to achieve in the ECHAM5/MPI-OM than in either the CCSM3 or CCSM4 models.

Yang et al. (2012a, b, c) identified the primary cause for the difference between the critical points predicted by the ECHAM5/MPI-OM and NCAR AOGCMs to be the sea ice and snow albedos assumed in these models, with their values being highest in the ECHAM5/MPI-OM, slightly lower in CCSM4 and much lower in CCSM3. The most recent evaluation by Rogers et al. (2013) of AOGCM model performance in reproducing the observed pan-Arctic sea-ice retreat between 1980–2008 has demonstrated that CCSM3 does better than ECHAM5. Follow-on analyses by Voigt and Abbot (2012) in which the sea ice and snow albedos in ECHAM5/MPI-OM were reduced to values close to those those in CCSM3 led to the conclusion that it was still easier to initiate a hard snowball Earth than in either CCSM3 or CCSM4, while disabling sea ice dynamics in this model was suggested to make initiation more difficult to achieve. These authors therefore concluded that the sea ice dynamics represented in ECHAM5/MPI-OM might be a further important reason for easier initiation of hard snowball Earth than in either of the NCAR models. Pierrehumbert et al. (2011) have provided a review of the issues raised in these primary sources.

Our purpose herein is to fully test the influence of incorporating more realistic Neoproterozoic continental configurations for both the Sturtian and Marinoan glaciations on the bifurcation point for initiation of a hard snowball Earth climate state in CCSM3. This will provide an additional point of inter-comparison with the results for the ECHAM5/MPI-OM since Voigt et al. (2011) have obtained the bifurcation point in the case of an approximate Sturtian continental configuration. This is a further step towards realistic snowball Earth simulations using the CCSM family of models. The goal is once more to find the greenhouse gas level (primarily CO_2) required to induce a Snowball Earth when the TSI is fixed to that appropriate for the Neoproterozoic, i.e. $0.94TSI_0$. The influence of aerosol on the results is also analysed in the present paper for the first time and is found to have non-negligible influence on the outcome as well.

CPD
9, 3615–3662, 2013

2 Model description and continental configurations

2.1 Model description

The Community Climate System Model version 3 employed in this work simulates four major components of the climate system, namely atmosphere, ocean, land surface processes and sea ice, and the respective model components are the Community Atmosphere Model version 3 (CAM3), the Parallel Ocean Program (POP, based on version 1.4.3), the Community Land Model version 3 (CLM3) and the Community Sea Ice Model version 5 (CSIM5). These four components are linked through a flux coupler (CPL6), with no flux corrections between the components (Collins et al., 2006a).

Both CAM3 and POP are 3-D general circulation models, which will be run at the recommended (for paleoclimate studies) low resolution of T31 (approximately $3.75^{\circ} \times 3.75^{\circ}$) and "gx3" (100 and 116 grid points in the zonal and meridional direction, respectively), and 26 levels and 25 levels in the vertical, respectively. CLM3, which considers dynamic vegetation (although not relevant here) and explicit river routing will be run on the same grid as CAM3. CSIM5 includes both thermodynamics and dynamics of the sea ice and it is always run on the same grid as that of the ocean in the coupled mode. The time steps for the atmosphere, ocean, land and sea ice components are 30, 80 (the default of 120 min. was used in initial test runs with the present day continental configuration, see below), 30 and 60 min, respectively. Fluxes are exchanged every 1 h between atmosphere, land and sea ice components, and 1 day between the ocean and other components.

2.2 Continental configurations

The same continental configurations, one for 720 Ma (Sturtian) constructed by Li et al. (2008) but slightly modified to increase connectivity of the land masses and the other for 570 Ma (approximate Marinoan) constructed by Dalziel (1997), as employed by Liu and Peltier (2010, 2011) are adopted here (see Fig. 4 below). There are three reasons why the 570 Ma continental configuration, rather than the 630 Ma configuration constructed by Li et al. (2008), is employed here. The first is that the 570 Ma continental configuration has been earlier employed by Hyde et al. (2000) which was the first to demonstrate the existence of soft snowball solutions in an AGCM (GENESIS 2). It will be useful to confirm the results obtained there by using an AOGCM. The second is that the 630 Ma continental configuration of Li et al. (2008) is not significantly different from the 720 Ma continental configuration in terms of its influence on climate since continental fragments are concentrated in low latitude in both time slices, while the 570 Ma continental configuration provides a more distinct alternative. The final reason is that the Gaskiers glaciation, which may also have been global in scale, occurred around 580 Ma.

The mean elevation of the topographically "flat" continents relative to sea surface is assumed to be ~ 400 m, also consistent with that in Liu and Peltier (2010, 2011) which is lower than the present day value (~ 740 m) but slightly higher than that (100 m) employed by Voigt et al. (2011). It has been commonly accepted that the mean continental elevation had been almost constant through geological time (e.g. Hynes, 2001), but a recent study (Lorentz, 2008) has challenged this view and proposed that the mean continental elevation could have been even higher during the Neoproterozoic. This issue is not expected to be settled anytime soon, but the most important thing relevant to the work to be presented here is that the difference in mean climate states obtained for 100 m and 400 m mean elevations is small, smaller than 0.5 °C in terms of globally averaged annual mean surface temperature. To assist in creation of the river routing map needed for the analyses we have performed, the elevation at the center of the individual continents is raised by 50 m and decreases linearly to 400 m towards the edges/envelope of the continents.

To set up the CCSM3 model for these realistic Neoproterozoic continental configurations, we have generally followed the instructions provided by the National Center for Atmospheric Research (NCAR) (Rosenbloom et al., 2009). The vegetation type on land is set to desert everywhere since surface vegetation has not yet significantly evolved by Neoproterozoic time. Soil color, which determines the dry and saturated soil albedo, is set to a medium value of 4 on a scale of 1 to 8 where 1 is the brightest (Oleson et al., 2004, technical report). The albedo of the soil (4) is 0.09–0.18 in the visible band and 0.18–0.36 in the near-infrared band depending on whether it is water saturated (corresponding to the low value) or dry (the high value). Soil texture which determines the soil thermal and hydrologic properties is set to be that of an average soil, consisting of ~ 15 % clay, 43 % sand and the rest silt. There are no lakes or wetlands assumed to exist on the land which would lower the effective albedo of the surface and therefore further impede the transition into the hard snowball regime.

In order for the ocean module, POP, to run properly, the poles of the ocean grid have to reside on land. But because there are no polar continental fragments in either of the continental reconstructions we employ that lie poleward of ~ 65° for the 720 Ma continental configuration or around the North Pole for the 570 Ma continental configuration, we have elected to introduce "fake" circular continents of radius 5° at the pole or poles as sites for the poles of the POP grid. This strategy is preferred because (1) it involves least stretch and distortion of the ocean grid, and (2) it is not expected to have a significant influence in determining the hard snowball bifurcation point since long before entering a hard snowball state, the polar and mid-latitude regions will already be covered by sea ice, therefore the ocean circulation within the polar region is expected to be weak. This has been partially demonstrated to be true in the analyses of modern snowball Earth initiation by Yang et al. (2012a, b, c).

To find the hard snowball bifurcation point, we need to have a control run for both continental configurations, a control run which has a relatively warm equilibrium climate. For this control run, we set the TSI to be $0.94\mathrm{TSI}_0$, $p\mathrm{CO}_2$ to be 2000 ppmv, aerosol optical depth ("tauback") to be 0.12, and $p\mathrm{CH}_4$ and $p\mathrm{N}_2\mathrm{O}$ to have pre-industrial values as described above. Both the atmosphere and the ocean are initiated from static states, with the initial ocean temperature horizontally uniform but vertically decreasing from 24 °C at the surface to 9 °C in the abyss. The salinity of the ocean is assumed to be uniform with a value of 35 psu. However, negligible difference was found when

CPD
9, 3615–3662, 2013

the salinity was increased to 45 psu (results not shown). When the control run reaches equilibrium (after 4000 yr), branch runs are initiated by decreasing pCO_2 with TSI fixed.

Unfortunately, because the ocean bottom is flat and there is no continent in the mid-latitudes of the NH for either the 720 Ma or the 570 Ma continental configuration, the westerly jet of the ocean in mid-latitudes of the Northern Hemisphere will become extremely intense (like the Antarctic circumpolar current (ACC) of the modern ocean) and eventually the ocean model would fail to converge. This problem cannot be eliminated by decreasing the time steps of the components of CCSM3, nor by increasing the bottom drag (a factor of 100 was tested) of the ocean. However, there are several other options available for the elimination of this problem, one is to add fictitious ocean bottom topography or to add some narrow meridionally oriented continental strips in mid-latitudes, another is to increase the tracer diffusivities of the ocean.

Adding narrow meridionally oriented continents in mid-latitudes is not preferred because this would be expected to influence the climate significantly insofar as sea ice transport is concerned and would make the control model useless for the later analyses we will be performing in which explicit continental ice sheets are introduced. We will show in what follows that the continental configuration does have significant influence on the sea ice transport.

We are then left with the possibilities of correcting for the otherwise overly intense zonal current in the Northern Hemisphere by either adding fictitious mid-ocean ridges or increasing tracer diffusivities. We first tested the response of the model to the addition of such fictitious ridges (referred to as the RIDGE method hereafter), examples of which are shown in Fig. 1. Both straight ridges of different height (Fig. 1a and c) and more complex present-day mid-ocean ridges (Fig. 1b) but with the ridges of the current Southern Hemisphere flipped to the north have been investigated. It was found that the addition of such ridges does postpone the onset of model instability, and the effect is stronger with higher ridges (results not shown). When the height of the straight ridge is 2 km, we were able to obtain a control run that reaches equilibrium. However, when branching off from this control run to obtain a colder climate, the model again failed to

CPD
9, 3615–3662, 2013

converge. The same occurred in the version of the model with the more complex set of ridges.

We did not further increase the height of the straight ridge because, although the mid-ocean ridges of the present-day ocean can be higher than 2 km, the distance between the top of the ridges and the ocean surface is usually approximately 3 km or more (Fig. 1d). Even considering the sea level drop of 800–1000 m due to land ice sheet formation during snowball Earth occurrence (e.g. Liu and Peltier, 2013), the distance is still around 2 km. Moreover, as will be shown below in Fig. 4, the influence of even a 2 km ridge on ocean currents and the transport of sea ice towards low latitudes is quite obvious. Therefore, the method upon which we have finally settled is to increase the horizontal tracer diffusivities of the ocean (referred to as DIF method). More specifically, we increase both the isopycnal diffusivity (variable "ah" in the model) and the thickness diffusivity (variable "ah_bolus" in the model) by a factor of 5. This factor was determined by Y. Shin (University of Toronto, personal communication, 2010) to be sufficient to stabilize the model in the context of aqua-planet simulations.

Since the default values for both diffusivities in CCSM3 at gx3 resolution are $800\,m^2\,s^{-1}$, the enhanced diffusivities in the DIF method here are then $4000\,m^2\,s^{-1}$. This or perhaps even higher values have been demonstrated to be appropriate for the regions where intense currents and thus intense baroclinic instability occurs, for example, around the region where intense westerlies are present (Ferreira et al., 2005). In the newer version of the NCAR model CCSM4, these two diffusivities have been formulated to be vertically varying depending on the stratification following Ferreira et al. (2005) and Danabasoglu and Marshall (2007). For the 3° resolution employed in the analyses reported herein, both diffusivities can be as large as $4000\,m^2\,s^{-1}$ in the upper ocean, but decreases to $300\,m^2\,s^{-1}$ by a depth of about 2000 m. In our simulations with a flat ocean bottom, very strong westerly ocean currents (zonal speed reaches $70\,cm\,s^{-1}$ and the width of the current in the meridional direction is approximately 20°, not shown) develop in the NH, especially for the 570 Ma continental configuration, warranting the employment of higher tracer diffusivities than the default. A drawback is that

CPD
9, 3615–3662, 2013

this high tracer diffusivity is applied uniformly to the ocean in CCSM3 which may have a significant influence on the ocean circulation. However, as will be described in what follows, employing high tracer diffusivities should not have significant influence on the hard snowball Earth bifurcation point. Tracer diffusivities as high as $4000\,m^2\,s^{-1}$ have also been employed by Poulsen et al. (2001) in their study of ocean dynamics during snowball Earth occurrence.

3 Impact of vegetation and aerosol

Many of the variables in the model, such as vegetation, ozone, CFCs, aerosols etc., are unconstrained or are known to have been very different from their present-day values during the Neoproterozoic, and must therefore be either simplified in their description or eliminated entirely. To test the degree to which the modification of these variables affects the climate, we choose to use the present-day continental configuration.

These tests turned out to be important because, as will be described in what follows, the continental vegetation and the nature of the atmospheric aerosol distribution have a significant influence on the climate through modification of the surface albedo and planetary albedo, respectively.

The series of simulations that were performed for the purpose of the above described investigations is listed in Table 1 in order of the increasing number of variables being modified. The first simulation was performed using the default configuration of CCSM3 which is appropriate for the year 1990; for example, pCO_2 and pCH_4 are 355 ppmv and 1714 ppbv, respectively, significantly higher than those for the pre-industrial period, and $TSI = TSI_0$. In the ensuing simulations 2–11, the following changes of variables are progressively introduced: ozone is changed from the distribution appropriate for present day climatology to the preindustrial distribution (Rosenbloom et al., 2009), vegetation is completely removed, lakes and wetlands are removed, soil color (which affects the albedo of dry and saturated soil) is changed to a uniform value of 4, soil texture is changed to that for an averaged soil ($\sim 15\,\%$ clay, $\sim 43\,\%$ sand and the rest silt), pCO_2

CPD
9, 3615–3662, 2013

The initiation of Neoproterozoic “snowball” climates in CCSM

Y. Liu et al.

is reduced to 300 ppmv, $p\mathrm{CH_4}$ is reduced to 0, $p\mathrm{N_2O}$ is reduced to 0, CFCs are removed, aerosol climatology is replaced by a time-invariable and spatially uniform layer which has an optical depth determined by the variable "tauback".

Most of these simulations were continued for only 100 yr in order to examine their short-term influence on the climate, and the results are shown in Fig. 2a. The time series of globally averaged annual mean surface temperature in this figure demonstrate that changing ozone, removing CFCs, and changing soil texture all have a slight ($< 0.3\,^{\circ}$C) cooling effect, while removing vegetation (black curve in Fig. 2a) has a significant cooling effect ($\sim 0.5\,^{\circ}$C in 100 yr). Both removing lakes and wetlands (green curve) and changing soil color (pink curve) after the vegetation already being removed seem to have a negligible effect on the climate. A major impact on the short-term global mean temperature, however, derives from the reduction of $p\mathrm{CO_2}$, $p\mathrm{CH_4}$, $p\mathrm{N_2O}$ and the change of the aerosol distribution, each of which cools the climate by $> 0.5\,^{\circ}$C in the short term. We must therefore pay greater attention to what might be the most appropriate Neoproterozoic values for $p\mathrm{CH_4}$, $p\mathrm{N_2O}$ and aerosol in our investigations of the hard snowball bifurcation point for the our realistic continental configurations. In order to have a better idea as to what values might be appropriate, we need to consider the longer-term influence on climate.

To this end Fig. 2b shows 2000 yr time series for global mean surface temperature for runs 11, 12, 13 and 16. Clearly, if both $p\mathrm{CH_4}$, $p\mathrm{N_2O}$ are removed and aerosol is replaced by a uniform layer with its tauback value (which determines the optical depth of the layer) set to be 0.28 as recommended in the instruction manual for paleoclimate studies provided by National Center for Atmospheric Research (NCAR) (Rosenbloom et al., 2009), the climate will be dramatically colder than that of present-day with the global mean surface temperature as low as $\sim 4\,^{\circ}$C (run 11, Fig. 2b). Since there are no constraints on these three variables for the Neoproterozoic, we will choose the pre-industrial values 805.6 ppbv and 276.7 ppbv for $p\mathrm{CH_4}$ and $p\mathrm{N_2O}$, respectively, to be consistent with Yang et al. (2012a, b, c). These are also the same values as those employed by Voigt and Marotzke (2010) but slightly higher than those ($p\mathrm{CH_4} = 650$ ppbv

CPD
9, 3615–3662, 2013

and pN_2O = 270 ppbv) employed by Voigt et al. (2011) in the ECHAM5/MPI-OM simulations. This will make comparison of the bifurcation points obtained here with those obtained in these previous studies more instructive.

For the choice of tauback, the issue is more subtle. A value of 0.28 was suggested by Rosenbloom et al. (2009) for deep paleoclimate studies, but clearly adopting this value will cause the climate to cool by more than 2 °C in the global mean surface temperature value (compare the result for run 13 which uses a value of 0.24 for tauback with run 12 which employs the present-day aerosol climatology in Fig. 2b, all other conditions remaining the same. Using a higher value for tauback such as 0.28 will cool the climate further). This value was preferred in an earlier version (CCM3) of CAM3, whereas in CAM3 or CCSM3 a spatio-temporally varying climatology for aerosol is used as an improvement. Heavens et al. (2012) did a sensitivity study for the Late Permian (251 Ma) with the CCSM4 model and found that the climate obtained with a uniform layer of aerosol with a tauback value of 0.28 is ~ 1.5 °C cooler than that obtained with a prescribed spatio-temporally varying aerosol. The global mean optical depth of their prescribed spatio-temporally varying aerosol, which itself was obtained by a prognostic model for aerosol, was only 0.08. Moreover, the global mean optical depth is only ~ 0.17 and 0.08 for the present-day and pre-industrial climates, respectively (Mahowald et al., 2011). Therefore, we have good reason to believe the tauback value of 0.28 is an overestimate of the optical depth appropriate for the Neoproterozoic climate simulations as well if the CCSM3 model is employed.

Run 12 (black curve in Fig. 2b) in which the pre-industrial pCH_4 and pN_2O and default aerosol climatology are used may serve as a reference simulation from which an appropriate value for tauback can be determined. The global mean surface temperature obtained in this run is ~ 11.2 °C, about 3.3 °C cooler than the present-day climate. The cooling is mainly due to the combined effects of removing vegetation, reducing pCH_4, changing soil texture and removing CFCs as discussed above. We found that a close to present-day climate can be obtained if the value of tauback is reduced to 0.12 (run 16 in Fig. 2b). Since there is no better constraint on this value, we will use both 0.28 and 0.12

in searching for the hard snowball bifurcation point for the Neoproterozoic continental configurations as a sensitivity test. Note that we may not completely rule out the high value because the Neoproterozoic climate is expected to be much drier than today due to its low temperature (see e.g. Fig. 4 of Yang et al., 2012b) and therefore the contribution of dust aerosol might have been more important than is the case today.

4 Control simulation and ocean circulation

The control simulations for both the 720 and 570 Ma continental configurations are shown in Fig. 3. They were obtained successfully for both the RIDGE and the DIF methods. The equilibrium state obtained by the DIF method is close to that delivered by application of the RIDGE method for both continental configurations. For the 720 Ma continental configuration, the DIF method produces colder surface climate (by $\sim 1.3\,^{\circ}$C in terms of global mean surface temperature, see Fig. 3a and also Table 2) than that from the RIDGE method, while for the 570 Ma continental configuration, it produces a slightly warmer (by $\sim 0.2\,^{\circ}$C, Fig. 3b, see also Table 2) surface climate. Hereafter we take the results from the RIDGE method as most physical (because no model parameters were modified relative to the default settings in CCSM3) and analyze the difference between these results and those obtained by the DIF method. The main purpose is to demonstrate that the DIF method should not have any significant influence on our determination of the hard snowball bifurcation point.

In Fig. 4, the sea ice thickness and velocity at equilibrium are shown for both methods for both continental configurations. Clearly the most significant difference between the two methods is that the sea ice extent in the Southern Hemisphere (SH) is much larger for the DIF method, which causes the surface temperature of the SH to be lower (Fig. 5a and d). However, the surface temperature of the Northern Hemisphere (NH) is higher for the DIF method especially for the 570 Ma continental configuration (Fig. 5d). The issue as to why the DIF method acts asymmetrically on the two hemispheres is interesting. A clue may be found from the heat transport in the atmosphere and ocean.

CPD
9, 3615–3662, 2013

The atmospheric heat transport does show some asymmetric changes (e.g. Fig. 5e) when switching from the RIDGE method to the DIF method. This change is such that more heat is transported to the SH and less to the NH, opposite to the change of surface temperature. While the ocean heat transport shows much larger changes (e.g. Fig. 5f) when switching from the RIDGE method to the DIF method, the sign is consistent with that of the surface temperature changes, decreasing in the SH and increasing in the NH.

Figure 6a and c shows the meridional overturning circulation (MOC) in the RIDGE method for the 720 and 570 continental configuration, respectively. The wind-driven subtropical cells (STCs) of the upper ocean are similar to the present-day ocean. A strong channel flow develops at the middle latitudes of the NH for both these configurations of the model. Meanwhile, there exists a strong, counterclockwise deep water cell from the mid-latitudes of the NH all the way to the high latitudes of the SH. Such a feature is similar to the present-day Earth and to that obtained in the Double Drake experiment of Ferreira et al. (2010) but with the NH and SH switched. It is clearly due to the so-called "Drake passage effect" (Toggweiler and Samuels, 1995; Toggweiler and Bjornsson, 2000), which is such that a zonal channel flow in one hemisphere enhances the deep-water formation in the other hemisphere. The effect is such that more heat is transported by the ocean to the hemisphere where deep water forms and that there is a significant net heat transport across the equator from one hemisphere to the other hemisphere, as shown in Fig. 5c and f. Atmospheric heat transport acts to partially compensate the ocean heat transport (Fig. 5b and e).

Because the 570 Ma continental configuration does not have any continental fragment further north than 25° N, the channel flow is much stronger than that of the 720 Ma continental configuration (not shown) and the deep water formation in the SH is also much stronger. Indeed, the deep water cell for the 570 Ma continental configuration (Fig. 6c) has a strength of ~ 60 Sverdrup (Sv) compared to ~ 35 Sv for the 720 Ma continental configuration (Fig. 6a). This is also the reason why switching from the RIDGE

CPD
9, 3615–3662, 2013

method for the control of the ocean circulation to the DIF method has a larger impact for the 570 Ma continental configuration as will be described further in what follows.

Comparison of Fig. 6c and d clearly indicates that the deep water formation process is greatly weakened due to the increased tracer diffusivities. This is expected since it has been known that increased isopycnal and eddy-induced diffusivities act to weaken the effect of the channel flow on deep water formation (e.g. Gnanadesikan et al., 2003, 2004). The weakening of deep water formation in the SH causes less heat to be transported to the SH (Fig. 5f) and thus the atmosphere there to be colder (Fig. 5d), while the effect on the NH is opposite. The compensation by the atmospheric heat transport is reduced (Fig. 5e) since the ocean heat transport is now more symmetric. The changes for the 720 Ma continental configuration are much less significant since it had weaker deep water formation in the RIDGE method. Therefore, the primary influence of enhanced tracer diffusivities on the climate system is to weaken the deep water formation process, and redirect ocean heat transport. The consequence is that the climate in the two hemispheres is more symmetric (red curves in Fig. 5a and d).

For the 570 Ma continental configuration, the asymmetric change in the two hemispheres almost completely compensates so that the global mean surface temperature stays almost the same as that predicted by the RIDGE method (Fig. 3b). While for the 720 Ma continental configuration, the cooling effect in the SH is similar but there is no obvious warming in the NH (Fig. 5a) so that the global mean surface temperature is $\sim 1.3\,^{\circ}$C lower than that predicted by the RIDGE method (Fig. 3b).

A significant question concerns the issue as to whether use of the DIF method will have a significant influence on the hard snowball bifurcation point? We expect not. As the Earth becomes increasingly close to entering a hard snowball state, the climate in the two hemispheres tends to be more and more symmetric (see Fig. 1b for the atmosphere and Fig. 2b for the ocean of Yang et al., 2012b) and the deep ocean circulation becomes less and less important, so that the influence of using the DIF method is therefore expected to be minimal. The fact that switching from the RIDGE method to the DIF method does not have any significant effect on either the NH surface temperature (Fig. 5a) or sea ice front position (compare Fig. 4a and b) for the 720 Ma continental configuration, may be taken as an analog for the influence of the DIF method on an already relatively symmetric climate. However, because the upper ocean circulation (Fig. 6) and ocean heat transport (Fig. 5c) are slightly enhanced in the tropical region when tracer diffusivities are increased, the DIF method might have a slight effect of preventing the advance of the sea ice fronts towards the equator once they enter the tropical region which is under the influence of the Hadley circulation.

5 Predictions of the impact of continental configuration on the Neoproterozoic hard snowball bifurcation point

Branch runs are initiated from the end of the control simulations obtained by applying the DIF method and results are shown in Figs. 7 and 8 for the 720 Ma and 570 Ma continental configurations, respectively. For these branch runs, the TSI is fixed at $0.94TSI_0$. As expected, the Earth enters a hard snowball state more easily than the present-day Earth as determined by Yang et al. (2012a,b) because of the cumulative cooling effect due to the removal of vegetation, lakes and wetlands, and changing soil color etc. as described previously. When the optical depth of the aerosol layer is set to a relatively low value (tauback = 0.12), the Earth enters a hard snowball state when $p\mathrm{CO_2}$ is reduced to between 50–60 ppmv (Fig. 7a) and 100–110 ppmv (Fig. 8a) for the 720 Ma and 570 Ma continental configurations, respectively. When the high value of 0.28 is employed, the Earth enters a hard snowball state at higher values of $p\mathrm{CO_2}$ between 80–90 ppmv (Fig. 7b) and 140–150 ppmv (Fig. 8b) for the two continental configurations, an increase of ∼ 50 % and 40 %, respectively. Clearly, the influence of paleogeography on hard snowball bifurcation point is significant, in fact comparable to that of the assumed optical depth of the aerosol layer. However, the influence of both of these influences may be considered small compared to the uncertainties in sea ice albedo and sea ice dynamics (e.g. Voigt and Abbot, 2012; Yang et al., 2012a, b, c).

CPD
9, 3615–3662, 2013

Maximum sea ice fraction (ratio of sea ice area over the global ocean area) obtained before entering a hard snowball is ∼ 55 % (cyan curves in Fig. 7) and ∼ 50 % (cyan curves in Fig. 8) for the 720 and 570 Ma continental configurations, respectively, much less than that obtained for the present-day continental configuration (∼ 75 %, Yang et al., 2012a,b) using the same model. This could be due to the increased ocean tracer diffusivities employed for the purpose of the analyses described in this paper. Our results of the maximum sea-ice fraction are similar to those obtained by Voigt et al. (2011) using the ECHAM5/MPI-OM model with the 635 Ma Marinoan continental configuration.

The sea ice front (defined by the grid-box sea ice fraction being equal to 50 %) generally reaches 24–27° N(S) and 27–30° N(S) for the 720 and 570 Ma continental configurations, respectively (results not shown, but see Fig. 9 for a close analog). However, the local sea ice front can reach as close as 15° N for the 720 Ma continental configuration (around 180° E in Fig. 9a) and 24° S for the 570 Ma continental configuration (around 50° W in Fig. 9b) due to the transport by the wind stresses. The seasonal cycle of the sea ice front is strong (result not shown), similar to that shown in Fig. 4 of Yang et al. (2012a). Although it has been described in Yang et al. (2012a) that the sea ice front can reach 10° S(N), this position is reached only seasonally. For the annual mean, the sea ice front reaches only ∼ 20° S and 15° N (again see their Fig. 4), still much closer to the equator than obtained here.

It is worth noting that the critical pCO_2 values obtained for the 720 Ma continental configuration may be underestimated since the simulations with higher pCO_2 values have yet to reach statistical equilibrium 3000 yr after the branch run was initiated. For example, the run with $pCO_2 = 60$ ppmv is still drifting very slowly towards colder climate at year 7000 (Fig. 7) and we cannot therefore rule out the possibility that it might eventually enter a hard snowball state. The runs for which $pCO_2 = 60$ ppmv in Fig. 7a (cyan curve) and $pCO_2 = 100$ ppmv in Fig. 7b (cyan curve) have been continued till year 9000, and since the Earth had not entered a hard snowball state by this time the runs were not continued further.

CPD
9, 3615–3662, 2013

As an effort to further quantify the influence of enhanced tracer diffusivities on the identification of bifurcation points, two simulations employing slightly lower values, 3200 and 2400 $m^2 s^{-1}$, were carried out for the 570 Ma continental configuration with $pCO_2 = 140$ ppmv. Compared to the simulation with tracer diffusivities of 4000 $m^2 s^{-1}$ (blue curve in Fig. 8a), the global mean surface temperature is lower by 0.14 and 0.23 °C, respectively. Therefore, enhanced tracer diffusivities do produce warmer climate due to enhanced ocean heat transport, thus leading to an underestimate of the critical pCO_2 for hard snowball Earth formation but the magnitude of this effect is small compared to other uncertainties of the model such as sea-ice albedo, sea-ice dynamics and cloud parameterization etc.

6 Discussion

Figure 10 illustrates the relationship between global mean surface temperature and pCO_2. Clearly, the global mean surface temperature decreases almost linearly with applied CO_2 forcing (note the logarithmic scale of the x-axis of Fig. 10) for both continental configurations. The trend is consistent with that found in Yang et al. (2012b) with the slope reaching approximately −6 K per halving of pCO_2 or $\sim 2.3\,K\,(W\,m^{-2})^{-1}$ if the forcing per halving of pCO_2 is assumed to be $-2.66\,W\,m^{-2}$ (Collins et al., 2006b). This high climate sensitivity is beyond the upper bound of the climate sensitivity (2.1–4.4 K per doubling of pCO_2, IPCC(AR4), 2007) obtained for present-day climate among different models, probably due to the action of larger sea ice and snow albedo feedback here because these characteristics of the model both extend into the tropical region. Also seen from Fig. 10 is the fact that, subject to the same radiative forcings (solar insolation and greenhouse gas concentrations), the 570 Ma climate is always colder than the 720 Ma climate. The difference in global mean surface temperature is very small (~ 0.5 °C) for the control run, but increases significantly to ~ 3.5 °C when pCO_2 is reduced to a concentration equal to or below 286 ppmv. This is perhaps surprising since it was expected that the relatively high albedo of (bare) land would have a stronger cool-

CPD
9, 3615–3662, 2013

ing effect when the continents are located at low latitude rather than at high latitude (e.g. Kirschvink, 1992). Therefore, there are clearly other internal processes that are acting more strongly than the radiative forcings due to land albedo, and it is instructive to identify these processes.

First, we find that the reason as to why the 570 Ma climate is colder than the 720 Ma climate differs significantly between the control runs ($p\mathrm{CO_2}$ = 2000 ppmv) and the branch runs ($p\mathrm{CO_2} \leq$ 286 ppmv). This is demonstrated in Fig. 11, which shows that the colder global mean surface temperature for the 570 Ma model is primarily due to much colder surface temperature in the South Polar region (90–60° S) for this continental configuration during austral winter (compare Fig. 11a and b). Albedo cannot play any significant role for this season since there is no sunlight. This difference in winter temperature between the two continental configurations is due to the higher heat capacity of the ocean compared to that of the land. During winter, the ocean in the South Polar region in the 720 Ma continental configuration is able to release a large amount of heat to the ocean surface and the overlying atmosphere, and the sensible heat flux to the atmosphere is almost 20 W m^{-2} larger than that for the 570 Ma continental configuration. Actually the sensible heat flux is negative for the 570 Ma configuration during the austral winter, i.e. the atmosphere loses heat to the snow covered land due to the existence of a temperature inversion. This should be a general feature independent of the numerical models employed. For the branch runs (that for $p\mathrm{CO_2}$ = 140 ppmv is an example) however, the surface temperature for the 570 Ma model is lower than that for the 720 Ma model in all seasons (Fig. 11c and d). The reasons for this are more complex and will be described in detail in what follows.

Figure 12 compares the zonal mean surface temperature, surface albedo, planetary albedo, water vapor content in the atmospheric column, mass stream function of the atmosphere at 500 hPa, net cloud forcing, sea ice mass change due to sea-ice transport, atmospheric and oceanic heat transports between the 720 and 570 Ma continental configurations. Clearly, the temperature difference around the South Pole is still much larger than other latitudinal regions of the Earth (Fig. 12a), but now the cooler temper-

CPD
9, 3615–3662, 2013

ature in the tropical region for the 570 Ma than for the 720 Ma continental configuration makes a significant contribution to the global mean surface temperature due to its large area. In the South Polar region, the difference in sensible heat flux between the 720 Ma and 570 Ma models is still playing a role but a less significant role than before due to the thick sea ice. The influence of albedo (both surface and planetary, see Fig. 12b and c) is now playing a more significant role in the southern part of the SH (90–60° S), but this difference in albedo between the two continental configurations is due to the contrast in the albedo of land snow (~ 0.8) and sea ice (and the snow on it, ~ 0.5) in CCSM3. This causes the surface temperature of 570 Ma configuration to be colder than the 720 Ma configuration during austral summer as shown in Fig. 10c. This feature may not be as significant in other models; for example, the sea ice albedo (0.75) in the standard version of ECHAM5/MPI-OM is comparable to the albedo of snow.

In the tropical-subtropical region, however, cloudiness is playing a significant role in contributing to the colder temperature of the 570 Ma model than 720 Ma model. Figure 12f clearly shows that the net cloud forcing for the 570 Ma model is more negative than for the 720 Ma model especially in the NH near the sea ice edge (which is near the region of steep slope of the surface albedo in Fig. 12b). This more negative cloud forcing for the 570 Ma continental configuration may be due to the greater ocean area near the ice edge in the northern tropical region (between 25° N and 30° N) so that the cloud (mainly the low cloud) coverage is higher as seen in Fig. 13. The reason is similar for the slightly less negative cloud forcing in the SH for the 570 Ma than 720 Ma model as shown Fig. 12f. Such a difference in cloud forcing is also present in the control runs but only in the SH since that is where the ocean fraction is different around the ice edges, and the forcing is actually more negative for the 720 Ma continental configuration. Within the region of 10° S–10° N, the stronger Hadley circulation for the 570 Ma configuration (see Fig. 12e which shows the mass stream function at 500 hPa) implies stronger convection, and thus greater cloudiness (compare Fig. 13c and d) despite the fact that the water vapor content in the atmo atmospheric column for this continental configuration is lower (Fig. 12d).

Although cloud parameterizations are very different among different GCMs (e.g. Wyant et al., 2006; Zhao, 2013a, b) we think this feature of more low cloud coverage and more negative cloud forcing near the ice edges when there is less continent in the tropical region is physically sound and expect it to be robust among models. Our results seem to be consistent in this regard with those from the ECHAM5/MPI-OM (Voigt and Marotzke, 2010). However, the strength of this impact is likely model dependent, as it has been shown that the cloud radiative forcing in a hard Snowball climate state is significantly different between models (Hu et al., 2011; Abbot et al., 2012).

There is obviously a fourth factor that also acts to cool the 570 Ma climate more than the 720 Ma climate; the sea ice front for the former is closer to the equator than for the latter as can be inferred from the surface albedo in Fig. 12b. The reason for this is illustrated by Fig. 12g, which shows that significantly more sea ice is transported to the ice edge in the Northern Hemisphere for the 570 Ma model than for the 720 Ma continental configuration. The primary reason for the enhanced sea-ice transport in the 570 Ma model is directly connected to the continental configuration in the Northern Hemisphere. Southward transport of sea ice in the Northern Hemisphere for the 720 Ma model is clearly partially blocked by the continents present in the mid-latitude region (compare Fig. 9a and b) while it is not for the 570 Ma continental configuration. The effect of continental obstruction of sea-ice transport is expected to be independent of the GCM model employed.

Our finding that high-latitude continents are more conducive to global glaciation contradicts the conclusion by Lewis et al. (2003) and Voigt et al. (2011). Voigt et al. (2011) came to their conclusion based on the simulation of results for a single Neoproterozoic continental configuration and compared it with the results for present-day geography (Voigt and Marotzke, 2010), however they did not quantify the cooling effect of removing vegetation. Furthermore, they have specified the albedo of land surface to be 0.272 uniformly, which is equivalent to the mean albedo for dry soil (0.18 for visible and 0.36 for the infrared) employed here. For water saturated soil, however, our albedo is reduced by half. Given the non-negligible precipitation on tropical land (not shown), the

CPD
9, 3615–3662, 2013
The initiation of Neoproterozoic “snowball” climates in CCSM
Y. Liu et al.

effective surface albedo in our model (∼ 0.18) is much lower than that employed by Voigt et al. (2011). Moreover, the sea ice albedo in ECHAM5/MPI-OM model employed by Voigt and Marotzke (2010) and Voigt et al. (2011) is much higher than that in the CCSM3 model (Yang et al., 2012b), which reduces the albedo contrast between sea ice (and the snow on it) and snow on land as observed in Fig. 12b. The model employed by Lewis et al. (2003) is an Earth system model of intermediate complexity, the University of Victoria (Uvic) model, in which all atmospheric dynamics are parameterized rather than explicitly resolved, and so it is unclear what might be the reason or reasons for the difference between their results and the results described herein.

Our finding of the cooling effect of land-snow albedo for the high-latitude continental configuration is consistent with that by Poulsen et al. (2002) who employed the AOGCM FOAM1.4, even though the sea ice albedo in FOAM (∼ 0.6) is higher than that (∼ 0.5) in CCSM3.

Figure 12h and i indicates that when $p\mathrm{CO_2}$ is relatively low, so that the sea-ice front reaches ∼ 30° N(S), the atmospheric and oceanic heat transports become more symmetric about the equator compared to the control run (Fig. 5c and f) and the difference between the 570 Ma and 720 Ma continental configurations becomes very small. This further suggests that when the climate is cold the DIF method will have a similar influence on the ocean circulation regardless of the continental configuration, unlike the circumstance in which the climate is relatively warm as described previously (Figs. 5 and 6).

7 Conclusion

We have studied in detail the hard snowball bifurcation point for two realistic Neoproterozoic continental configurations using CCSM3, which is a further improvement on this subject relative to the work of Yang et al. (2012a,b) who employed the present-day continental configuration. The bifurcation point is highly dependent on the parameterization of the optical depth of aerosol, the variable “tauback” in the CCSM3 model.

CPD
9, 3615–3662, 2013

When a larger value, 0.28, is adopted, the critical values of pCO_2, below which a hard snowball will be realized, are between 80–90 ppmv and 140–150 ppmv for the 720 and 570 Ma continental configurations, respectively. However, if a lower value, 0.12, which approximately reproduces the present-day climate (in terms of global mean surface temperature), the critical values of pCO_2 become 50–60 ppmv and 100–110 ppmv for the two continental configurations, respectively. For either case, they are higher than the values obtained by Yang et al. (2012a, b) primarily due to the absence of vegetation during the Neoproterozoic and the consequent higher surface albedo of continental surfaces. These values are nevertheless much lower than those obtained using the ECHAM5/MPI-OM model in its standard configuration (∼ 500 ppmv, Voigt et al., 2011), and still somewhat lower than the values obtained when the sea ice albedo in that model is reduced from 0.75 to a more appropriate value of 0.45 (∼ 204 ppmv, Voigt and Abbot, 2012) for the reasons that we have previously explained in Yang et al. (2012a, b, c). The remaining difference may be due to the significant difference in sea-ice dynamics between the two models (Voigt and Abbot, 2012), but the present study suggests that this could also be due in part to the different parameterization of aerosols. These new results are similar to those obtained previously using CCSM4 but with the present-day continents (70–100 ppmv) (Yang et al., 2012c).

The high-latitude continental configuration (570 Ma) is found to be more conducive to global glaciation than the low-latitude continent distribution (720 Ma) in the CCSM3 model. Four factors contribute to the cooler climate of the 570 Ma configuration: the low heat capacity of land in southern high-latitudes of the 570 Ma continental configuration produces much colder local winter temperature than does the 720 Ma continental configuration; the higher albedo of land snow cover compared to that of sea ice also makes the SH of the 570 Ma model colder than that of the 720 Ma model; furthermore, the cloud forcing in the NH is more negative within the tropical region in the 570 Ma configuration than in the 720 Ma configuration; and finally the sea ice in the NH of the 570 Ma model can be transported towards the equator more easily than that in the 720 Ma model because there is increased continental cover able to impede the south-

CPD
9, 3615–3662, 2013

ward transport of sea ice in the latter configuration. Among the four factors, the first factor is the least important since it creates little difference in global mean temperature between the two continental configurations when $pCO_2 = 2000$ ppmv (Fig. 10). The second factor should have a smaller influence than the third and fourth since it mainly affects the mid- to high-latitudes of the SH only.

In the interpretation of the meaningfulness of these computations of the hard snowball bifurcation point, it will be important to keep in mind the fact that an additional negative feedback which acts through the agency of the ocean carbon cycle could entirely eliminate the existence of such a bifurcation point. Peltier et al. (2007) have suggested that as the climate system begins to cool towards a transition of this kind a strong drawdown of oxygen into the ocean would occur as a consequence of its increasing solubility as temperature decreases. Since the Neoproterozoic ocean is expected to be especially rich in dissolved organic carbon the increased ventilation of the oceans would lead to the remineralization of this organic reservoir, the result being rapid production of carbon dioxide. Since part of this additional carbon dioxide would be exhausted into the atmosphere, the result would be a negative feedback through an enhancement of the greenhouse effect that would act to arrest the cooling towards the snowball bifurcation point and perhaps entirely eliminate the possibility of hard snowball Earth occurrence.

Acknowledgements. The required computations were performed on the SciNet facility at the University of Toronto, which is a component of the Compute Canada HPC platform. Y. Liu is very grateful to Christina Shields of NCAR for her help with a number of model related issues. Y. Liu has also greatly benefited from discussions with R. Toggweiler, R. Hallberg, A. Adcroft, S. Griffies Y. Zhang, M. Zhao and C. Golaz at GFDL. J. Yang thanks Dorian S. Abbot for his support. The research of WRP at Toronto is supported by NSERC Discovery Grant A9627.

References

Abbot, D. S., Voigt, A., Branson, M., Pierrehumbert, R. T., Pollard, D., Le Hir, G., and Koll, D. D. B.: Clouds and snowball Earth deglaciation, Geophys. Res. Lett., 39, L20711, doi:10.1029/2012gl052861, 2012.

Allen, P. A. and Etienne, J. L.: Sedimentary challenge to Snowball Earth, Nat. Geosci., 1, 817–825, doi:10.1038/Ngeo355, 2008.

Budyko, M. I.: Effect of solar radiation variations on climate of Earth, Tellus, 21, 611–619, 1969.

Chandler, M. A. and Sohl, L. E.: Climate forcings and the initiation of low-latitude ice sheets during the Neoproterozoic Varanger glacial interval, J. Geophys. Res.-Atmos., 105, 20737–20756, doi:10.1029/2000jd900221, 2000.

Collins, W. D., Bitz, C. M., Blackmon, M. L., Bonan, G. B., Bretherton, C. S., Carton, J. A., Chang, P., Doney, S. C., Hack, J. J., Henderson, T. B., Kiehl, J. T., Large, W. G., McKenna, D. S., Santer, B. D., and Smith, R. D.: The Community Climate System Model version 3 (CCSM3), J. Climate, 19, 2122–2143, doi:10.1175/Jcli3761.1, 2006a.

Collins, W. D., Ramaswamy, V., Schwarzkopf, M. D., Sun, Y., Portmann, R. W., Fu, Q., Casanova, S. E. B., Dufresne, J. L., Fillmore, D. W., Forster, P. M. D., Galin, V. Y., Gohar, L. K., Ingram, W. J., Kratz, D. P., Lefebvre, M. P., Li, J., Marquet, P., Oinas, V., Tsushima, Y., Uchiyama, T., and Zhong, W. Y.: Radiative forcing by well-mixed greenhouse gases: estimates from climate models in the Intergovernmental Panel on Climate Change (IPCC) Fourth Assessment Report (AR4), J. Geophys. Res.-Atmos., 111, D14317, doi:10.1029/2005jd006713, 2006b.

Corsetti, F. A., Olcott, A. N., and Bakermans, C.: The biotic response to Neoproterozoic snowball earth, Palaeogeogr. Palaeocl., 232, 114–130, doi:10.1016/J.Palaeo.2005.10.030, 2006.

Crowley, T. J., Hyde, W. T., and Peltier, W. R.: CO_2 levels required for deglaciation of a "Near-Snowball" Earth, Geophys. Res. Lett., 28, 283–286, doi:10.1029/2000gl011836, 2001.

Dalziel, I. W. D.: Neoproterozoic-Paleozoic geography and tectonics: review, hypothesis, environmental speculation, Geol. Soc. Am. Bull., 109, 16–42, 1997.

Danabasoglu, G. and Marshall, J.: Effects of vertical variations of thickness diffusivity in an ocean general circulation model, Ocean. Model., 18, 122–141, doi:10.1016/J.Ocemod.2007.03.006, 2007.

Deblonde, G. and Peltier, W. R.: A model of late Pleistocene ice sheet growth with realistic geography and simplified cryodynamics and geodynamics, Clim. Dynam., 5, 103–110, 1990.

Deblonde, G. and Peltier, W. R.: Simulations of continental ice-sheet growth over the last glacial–interglacial cycle – experiments with a one-level seasonal energy-balance model including realistic geography, J. Geophys. Res.-Atmos., 96, 9189–9215, 1991.

Donnadieu, Y., Fluteau, F., Ramstein, G., Ritz, C., and Besse, J.: Is there a conflict between the Neoproterozoic glacial deposits and the snowball Earth interpretation: an improved understanding with numerical modeling, Earth Planet. Sc. Lett., 208, 101–112, doi:10.1016/S0012-821x(02)01152-4, 2003.

Donnadieu, Y., Ramstein, G., Fluteau, F., Roche, D., and Gonopolski, A.: The impact of atmospheric and oceanic heat transport on the sea-ice instability during the Neoproterozoic, Clim. Dynam., 22, 293–306, 2004.

Ferreira, D., Marshall, J., and Heimbach, P.: Estimating eddy stresses by fitting dynamics to observations using a residual-mean ocean circulation model and its adjoint, J. Phys. Oceanogr., 35, 1891–1910, doi:10.1175/Jpo2785.1, 2005.

Ferreira, D., Marshall, J., and Campin, J. M.: Localization of deep water formation: role of atmospheric moisture transport and geometrical constraints on ocean circulation, J. Climate, 23, 1456–1476, doi:10.1175/2009jcli3197.1, 2010.

Gnanadesikan, A., Slater, R. D., and Samuels, B. L.: Sensitivity of water mass transformation and heat transport to subgridscale mixing in coarse-resolution ocean models, Geophys. Res. Lett., 30, 1967, doi:10.1029/2003gl018036, 2003.

Gnanadesikan, A., Dunne, J. P., Key, R. M., Matsumoto, K., Sarmiento, J. L., Slater, R. D., and Swathi, P. S.: Oceanic ventilation and biogeochemical cycling: Understanding the physical mechanisms that produce realistic distributions of tracers and productivity, Global Biogeochem. Cy., 18, GB4010, doi:10.1029/2003gb002097, 2004.

Gough, D. O.: Solar interior structure and luminosity variations, Sol. Phys., 74, 21–34, doi:10.1007/Bf00151270, 1981.

Heavens, N. G., Shields, C. A., and Mahowald, N. M.: A paleogeographic approach to aerosol prescription in simulations of deep time climate, J. Adv. Model. Earth Sy., 4, M11002, doi:10.1029/2012ms000166, 2012.

Hoffman, P. F. and Li, Z. X.: A palaeogeographic context for Neoproterozoic glaciation, Palaeogeogr. Palaeocl., 277, 158–172, doi:10.1016/J.Palaeo.2009.03.013, 2009.

Hoffman, P. F., Kaufman, A. J., Halverson, G. P., and Schrag, D. P.: A Neoproterozoic snowball earth, Science, 281, 1342–1346, 1998.

CPD
9, 3615–3662, 2013

The initiation of Neoproterozoic “snowball” climates in CCSM

Y. Liu et al.

Hu, Y., Yang, J., Ding, F., and Peltier, W. R.: Model-dependence of the CO_2 threshold for melting the hard Snowball Earth, Clim. Past, 7, 17–25, doi:10.5194/cp-7-17-2011, 2011.

Hyde, W. T., Crowley, T. J., Baum, S. K., and Peltier, W. R.: Neoproterozoic “snowball Earth” simulations with a coupled climate/ice-sheet model, Nature, 405, 425–429, 2000.

Hynes, A.: Freeboard revisited: continental growth, crustal thickness change and Earth’s thermal efficiency, Earth Planet. Sc. Lett., 185, 161–172, doi:10.1016/S0012-821x(00)00368-X, 2001.

IPCC: Climate Change 2007: The Physical Science Basis. Contribution of Working Group I to the Fourth Assessment Report of the Intergovernmental Panel on Climate Change, edited by: Solomon, S., Qin, D., Manning, M., Chen, Z., Marquis, M., Averyt, K. B., Tignor, M., and Miller, H. L., Cambridge University Press„ Cambridge, United Kingdom and New York, NY, USA., 2007

Jenkins, G. S. and Frakes, L. A.: GCM sensitivity test using increased rotation rate, reduced solar forcing and orography to examine low latitude glaciation in the Neoproterozoic, Geophys. Res. Lett., 25, 3525–3528, doi:10.1029/98gl52588, 1998.

Jenkins, G. S. and Smith, S. R.: GCM simulations of Snowball Earth conditions during the late Proterozoic, Geophys. Res. Lett., 26, 2263–2266, doi:10.1029/1999gl900538, 1999.

Kirschvink, J. L.: Late Proterozoic low latitude glaciation: the snowball Earth, in: The Proterozoic Biosphere: a Multi-Disciplinary Study, edited by: Schopf, J. W., Klein, C., and Des Maris, D., Cambridge University Press, Cambridge, 51–52, 1992.

Lewis, J. P., Weaver, A. J., Johnston, S. T., and Eby, M.: Neoproterozoic “snowball Earth”: dynamic sea ice over a quiescent ocean, Paleoceanography, 18, 1092, doi:10.1029/2003pa000926, 2003.

Li, Z. X., Bogdanova, S. V., Collins, A. S., Davidson, A., De Waele, B., Ernst, R. E., Fitzsimons, I. C. W., Fuck, R. A., Gladkochub, D. P., Jacobs, J., Karlstrom, K. E., Lu, S., Natapov, L. M., Pease, V., Pisarevsky, S. A., Thrane, K., and Vernikovsky, V.: Assembly, configuration, and break-up history of Rodinia: a synthesis, Precambrian Res., 160, 179–210, doi:10.1016/J.Precamres.2007.04.021, 2008.

Liu, Y. and Peltier, W. R.: A carbon cycle coupled climate model of Neoproterozoic glaciation: influence of continental configuration on the formation of a “soft snowball”, J. Geophys. Res.-Atmos., 115, D17111, doi:10.1029/2009jd013082, 2010.

Liu, Y. and Peltier, W. R.: A carbon cycle coupled climate model of Neoproterozoic glaciation: explicit carbon cycle with stochastic perturbations, J. Geophys. Res.- Atmos., 116, D02125, doi:10.1029/2010jd015128, 2011.
Liu, Y. and Peltier, W. R.: Sea level variations during snowball earth formation and evolution (part II): the influence of Earth rotation, J. Geophys. Res., submitted, 2013.
Lorentz, N. J.: On protracted Laurentian rifting, continental freeboard, and cap carbonates in Neoproterozoic time, Ph.D. thesis of Philosophy, University of Southern California, Ann Arbor, MI, 168 pp., 2008.
Mahowald, N., Ward, D. S., Kloster, S., Flanner, M. G., Heald, C. L., Heavens, N. G., Hess, P. G., Lamarque, J. F., and Chuang, P. Y.: Aerosol impacts on climate and biogeochemistry, Annu. Rev. Env. Resour., 36, 45–74, doi:10.1146/Annurev-Environ-042009-094507, 2011.
North, G. R., Mengel, J. G., and Short, D. A.: Simple energy-balance model resolving the seasons and the continents – application to the astronomical theory of the Ice Ages, J. Geophys. Res.-Oc. Atm., 88, 6576–6586, doi:10.1029/Jc088ic11p06576, 1983.
Oleson, K. W., Dai, Y., Bonan, G., Bosilovich, M., Dickinson, R. E., Dirmeyer, P., Hoffman, F., Houser, P., Levis, S., Niu, G.-Y., Thornton, P., Vertenstein, M., Yang, Z.-L., and Zeng, X.: Technical description of the Community Land Model (CLM), NCAR Technical Note, NCAR/TN-495+STR, 174, doi:10.5065/D6N877R0, 2004.
Peltier, W. R., Tarasov, L., Vettoretti, G., and Solheim, L. P.: Climate dynamics in deep time: modeling the "snowball bifurcation" and assessing the plausibility of its occurrence, in: The Extreme Proterozoic: Geology, Geochemistry, and Climate, edited by: Jenkins, G. S., McMenamin, M. A. S., McKay, C. P., and Sohl, L., Geophysical Monography, American Geophysical Union, Washington DC, 107–124, 2004.
Peltier, W. R., Liu, Y. G., and Crowley, J. W.: Snowball Earth prevention by dissolved organic carbon remineralization, Nature, 450, 813–818, doi:10.1038/Nature06354, 2007.
Pierrehumbert, R. T., Abbot, D. S., Voigt, A., and Koll, D.: Climate of the Neoproterozoic, Annu. Rev. Earth Pl. Sc., 39, 417–460, doi:10.1146/Annurev-Earth-040809-152447, 2011.
Pollard, D. and Kasting, J. F.: Snowball Earth: a thin-ice solution with flowing sea glaciers, J. Geophys. Res.-Oceans, 110, C07010, doi:10.1029/2004jc002525, 2005.
Poulsen, C. J. and Jacob, R. L.: Factors that inhibit snowball Earth simulation, Paleoceanography, 19, PA4021, doi:10.1029/2004pa001056, 2004.

CPD
9, 3615–3662, 2013

Poulsen, C. J., Pierrehumbert, R. T., and Jacob, R. L.: Impact of ocean dynamics on the simulation of the Neoproterozoic “snowball Earth”, Geophys. Res. Lett., 28, 1575–1578, doi:10.1029/2000gl012058, 2001.

Poulsen, C. J., Jacob, R. L., Pierrehumbert, R. T., and Huynh, T. T.: Testing paleogeographic controls on a Neoproterozoic snowball Earth, Geophys. Res. Lett., 29, 1515, doi:10.1029/2001gl014352, 2002.

Rogers, T. S., Walsh, J. E., Rupp, T. S., Brigham, L. W., and Sfraga, M.: Future Arctic marine access: analysis and evaluation of observations, models, and projections of sea ice, The Cryosphere, 7, 321–332, doi:10.5194/tc-7-321-2013, 2013.

Rosenbloom, N., Shields, C. A., Brady, E., Yeager, S., and Levis, S.: Using CCSM3 for Paleoclimate Applications, NCAR Technical Note, NCAR/TN-483+STR, 81, doi:10.5065/D69S1P09, 2011.

Runnegar, B.: Loophole for snowball Earth, Nature, 405, 403–404, doi:10.1038/35013168, 2000.

Sellers, W. D.: A global climatic model based on energy balance of the Earth–atmosphere system, J. Appl. Meteorol., 8, 392–400, 1969.

Toggweiler, J. R. and Bjornsson, H.: Drake Passage and palaeoclimate, J. Quaternary Sci., 15, 319–328, doi:10.1002/1099-1417(200005)15:4<319::AID-JQS545>3.0.CO;2-C, 2000.

Toggweiler, J. R. and Samuels, B.: Effect of Drake passage on the global thermohaline circulation, Deep-Sea Res. Pt. I, 42, 477–500, doi:10.1016/0967-0637(95)00012-U, 1995.

Tziperman, E., Abbot, D. S., Ashkenazy, Y., Gildor, H., Pollard, D., Schoof, C. G., and Schrag, D. P.: Continental constriction and oceanic ice-cover thickness in a snowball-Earth scenario, J. Geophys. Res.-Oceans, 117, C05016, doi:10.1029/2011jc007730, 2012.

Voigt, A. and Abbot, D. S.: Sea-ice dynamics strongly promote Snowball Earth initiation and destabilize tropical sea-ice margins, Clim. Past, 8, 2079–2092, doi:10.5194/cp-8-2079-2012, 2012.

Voigt, A. and Marotzke, J.: The transition from the present-day climate to a modern snowball Earth, Clim. Dynam., 35, 887–905, doi:10.1007/S00382-009-0633-5, 2010.

Voigt, A., Abbot, D. S., Pierrehumbert, R. T., and Marotzke, J.: Initiation of a Marinoan Snowball Earth in a state-of-the-art atmosphere–ocean general circulation model, Clim. Past, 7, 249–263, doi:10.5194/cp-7-249-2011, 2011.

Wyant, M. C., Bretherton, C. S., Bacmeister, J. T., Kiehl, J. T., Held, I. M., Zhao, M., Klein, S. A., and Soden, B. J.: A comparison of low-latitude cloud properties and their response to climate

CPD

9, 3615–3662, 2013

The initiation of Neoproterozoic “snowball” climates in CCSM

Y. Liu et al.

change in three AGCMs sorted into regimes using mid-tropospheric vertical velocity, Clim. Dynam., 27, 261–279, doi:10.1007/S00382-006-0138-4, 2006.
Yang, J., Peltier, W. R., and Hu, Y. Y.: The Initiation of modern "soft snowball" and "hard snowball" climates in CCSM3. Part I: the influences of solar luminosity, CO_2 concentration, and the sea ice/snow albedo parameterization, J. Climate, 25, 2711–2736, doi:10.1175/Jcli-D-11-00189.1, 2012a.
Yang, J., Peltier, W. R., and Hu, Y. Y.: The initiation of modern "soft snowball" and "hard snowball" climates in CCSM3. Part II: climate dynamic feedbacks, J. Climate, 25, 2737–2754, doi:10.1175/Jcli-D-11-00190.1, 2012b.
Yang, J., Peltier, W. R., and Hu, Y.: The initiation of modern soft and hard Snowball Earth climates in CCSM4, Clim. Past, 8, 907–918, doi:10.5194/cp-8-907-2012, 2012c.
Zhao, M.: An investigation of the connections between convection, clouds and climate sensitivity in a global climate model. Part I: diagnostic approach and cloud sensitivity in present-day simulations, J. Climate, submitted, 2013a.
Zhao, M.: An investigation of the connections between convection, clouds and climate sensitivity in a global climate model. Part II: cloud response to uniform SST warming, J. Climate, submitted, 2013b.

CPD
9, 3615–3662, 2013

Table 1. Summary of runs carried out with the present-day continental configuration in order to test the influence of variable changes. Variable "tauback" is the optical depth of aerosols. Characters "D", "R", "uni." and "–", stand for "default", "removed", "uniform" and "not applicable", respectively, where the default value (in the brackets) may follow the character "D".

Runs	Ozone	Veg	Lake	Soil color	Soil texture	pCO_2 (ppmv)	pCH_4 (ppbv)	pN_2O (ppbv)	CFCs	tauback
1	D	D	D	D	D	D(355)	D(1714)	D(311)	D	–
2	uni.	D	D	D	D	D(355)	D(1714)	D(311)	D	–
3	uni.	R	D	D	D	D(355)	D(1714)	D(311)	D	–
4	uni.	R	R	D	D	D(355)	D(1714)	D(311)	D	–
5	uni.	R	R	4	D	D(355)	D(1714)	D(311)	D	–
6	uni.	R	R	4	loam	D(355)	D(1714)	D(311)	D	–
7	uni.	R	R	4	loam	300.0	D(1714)	D(311)	D	–
8	uni.	R	R	4	loam	300.0	0	D(311)	D	–
9	uni.	R	R	4	loam	300.0	0	0	D	–
10	uni.	R	R	4	loam	300.0	0	0	R	–
11	uni.	R	R	4	loam	300.0	0	0	R	0.28
12	uni.	R	R	4	loam	300.0	805.6	276.7	D	–
13	uni.	R	R	4	loam	300.0	805.6	276.7	D	0.24
14	uni.	R	R	4	loam	300.0	805.6	276.7	D	0.20
15	uni.	R	R	4	loam	300.0	805.6	276.7	D	0.16
16	uni.	R	R	4	loam	300.0	805.6	276.7	D	0.12

CPD
9, 3615–3662, 2013

Table 2. Summary of the results of runs. $T_{present}$ is the annually averaged global mean surface temperature obtained at equilibrium under preindustrial solar insolation and greenhouse gas concentrations, i.e. $TSI = TSI_0$, $pCO_2 = 286.2$ ppmv. $T_{control}$ is similar to $T_{present}$ except that it is obtained for $TSI = 0.94 TSI_0$, $pCO_2 = 2000$ ppmv, i.e. the control simulations shown in Fig. 3. Critical pCO_2 indicates the value of pCO_2 for which the climate will enter a hard snowball state. This value is only determined to the precision of 10 ppmv. "RIDGE" indicates that a straight ridge of 2 km is added to the ocean floor (see Fig. 4 for their width and locations); "DIF" indicates that ocean bottom is flat but the bottom drag and tracer diffusivities are enhanced (see text).

	720 Ma			570 Ma		
	RIDGE	DIF Tauback = 0.12	DIF Tauback = 0.28	RIDGE	DIF Tauback = 0.12	DIF Tauback = 0.28
$T_{present}$ (°C)	–	13.2	10.6	–	12.7	9.5
$T_{control}$ (°C)	14.1	12.8	–	12.2	12.4	–
Critical pCO_2 (ppmv)	–	50–60	80–90	–	100–110	140–150

Discussion Paper | Discussion Paper | Discussion Paper | Discussion Paper |
CPD
9, 3615–3662, 2013
The initiation of Neoproterozoic "snowball" climates in CCSM
Y. Liu et al.

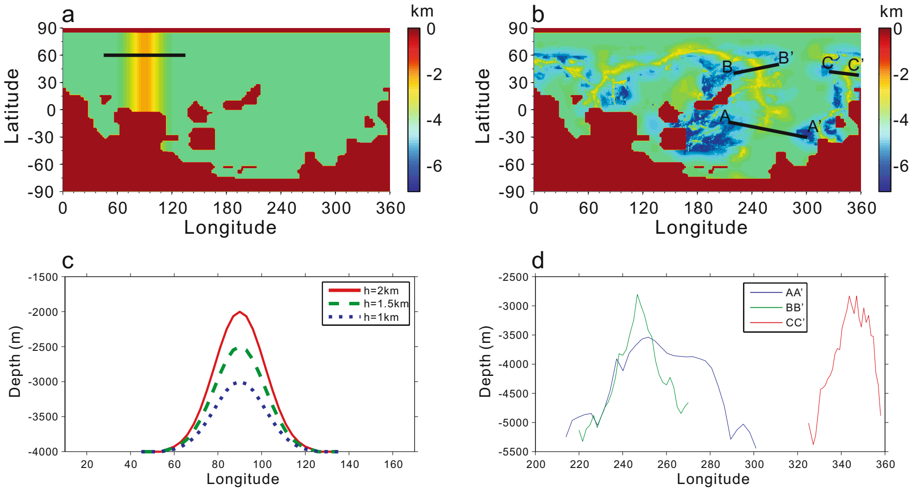

Fig. 1. Ocean bathymetry for 570 Ma with **(a)** simple straight and **(b)** present-day (with north and south flipped) mid-ocean ridges added. The straight ridge assumes the shape of a Gaussian function, with its width fixed but the height may vary from among 1.0, 1.5 and 2.0 km, as shown in **(c)**. The shape and heights of the cross section of present-day ridges are shown in **(d)**. The patches in dark red color in **(a)** and **(b)** are the continents.

CPD
9, 3615–3662, 2013

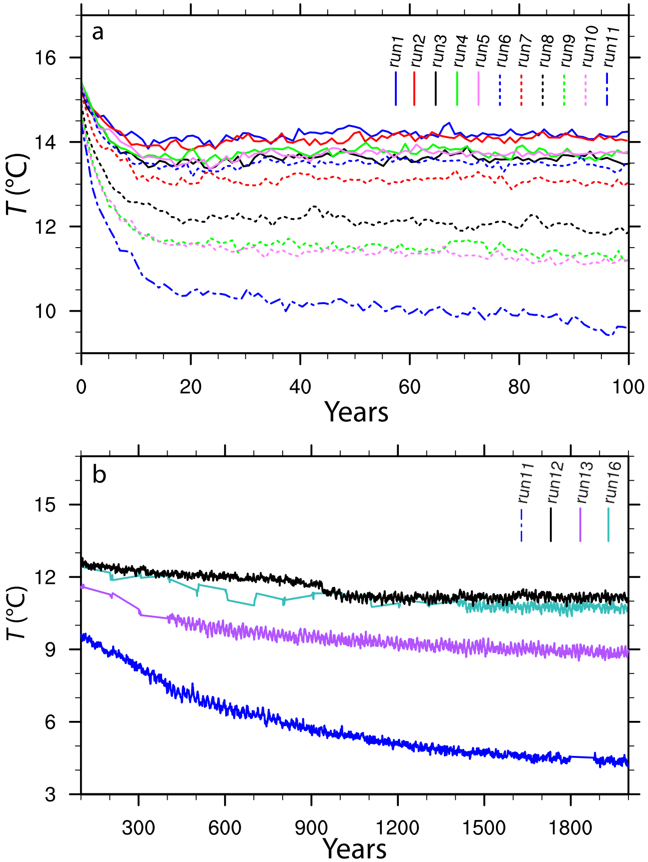

Fig. 2. Time series of annually averaged global mean surface temperature obtained for the test runs as listed in Table 1. **(a)** and **(b)** show the short-term and extended runs, respectively. For part of the long runs 11, 13 and 16, only 10 yr of results were retained for every 100 yr and they were connected by straight lines in order to make continuous curves.

CPD
9, 3615–3662, 2013

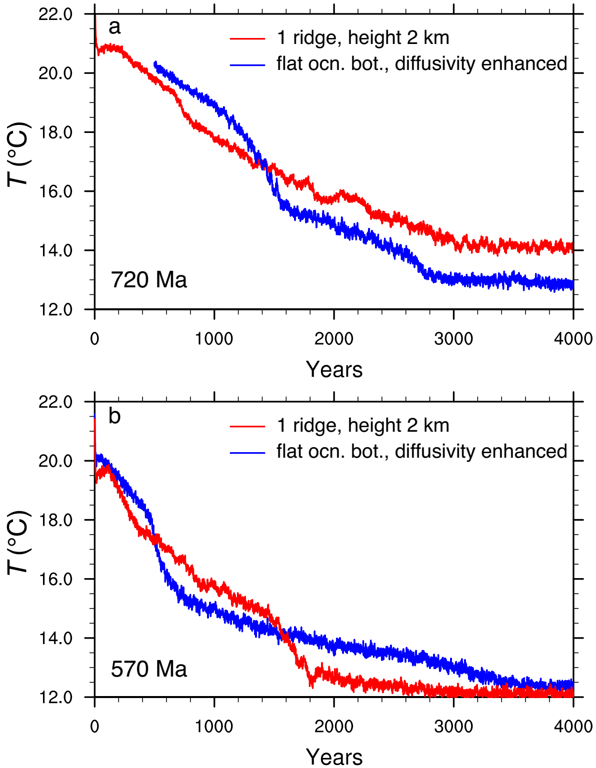

Fig. 3. Time series of global mean surface temperature of the control simulations for both **(a)** 720 Ma and **(b)** 570 Ma continental configurations. TSI is 94 % TSI_0, pCO_2 is 2000 ppmv, tauback is 0.12 for all four runs. The red curves are obtained for the model in which a straight ridge (e.g. Fig. 1) of height 2 km is added to the ocean bottom (i.e. the RIDGE method), while the blue curves are obtained for flat ocean bottom but bottom drag is increased by a factor of 100 and the isopycnal and thickness diffusivities are increased by a factor of 5 (the DIF method). The blue curves will be used as the control simulation from the end of which branch runs are started.

CPD
9, 3615–3662, 2013

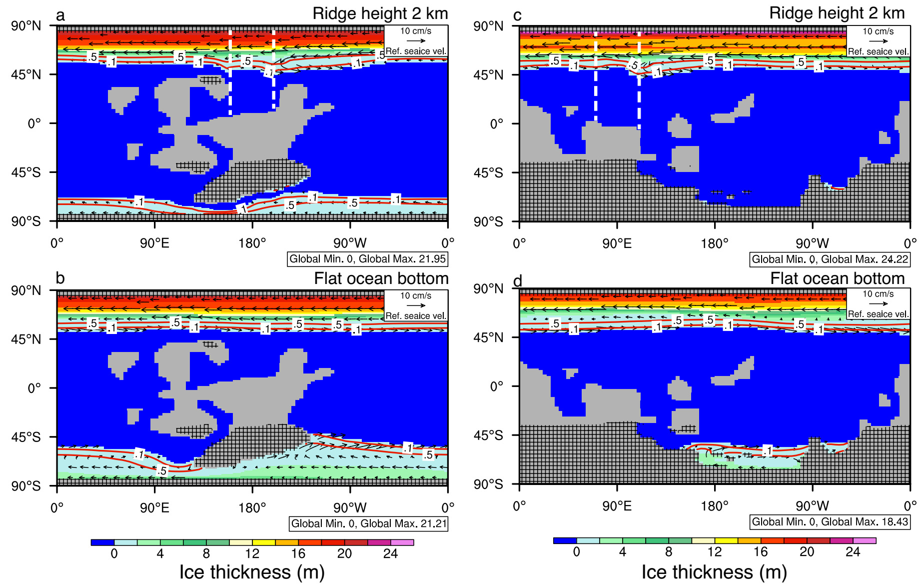

Fig. 4. Hundred-year mean sea ice thickness (filled contours) and velocity (arrows) obtained at the end of control runs (as shown in Fig. 3, for which TSI = $0.94\mathrm{TSI}_0$, $p\mathrm{CO}_2$ = 2000 ppmv) for the 720 Ma (**a** and **b**) and 570 Ma (**c** and **d**) continental configurations. A straight ridge (bounded by the white lines) of height 2 km is added to the ocean floor (i.e. the RIDGE method is applied) in **(a)** and **(c)**, while bottom drag and tracer diffusivities are enhanced (the DIF method is applied) in **(b)** and **(d)**. The grey area is the continent and the hatched regions represent land snow thicker than 1 cm. All sea ice with grid-box fraction greater than 1 % is plotted, but the contour lines (red curves) for grid-box fraction of 10 and 50 % are also superimposed.

CPD
9, 3615–3662, 2013

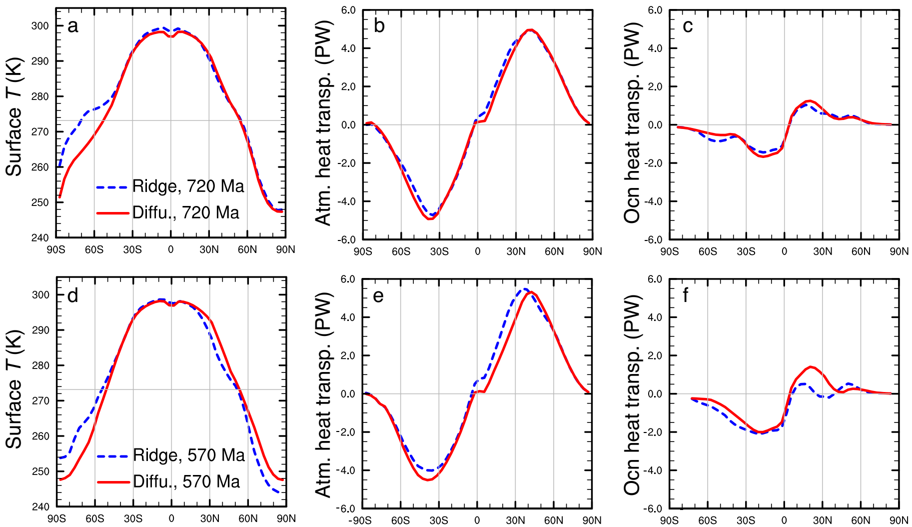

Fig. 5. Comparison of zonal mean surface temperature (**a** and **d**), atmospheric (**b** and **e**) and oceanic (**c** and **f**) heat transport obtained by employment of the RIDGE method (see Figs. 1 and 4) and of the DIF method. Upper and lower panels show results for the 720 and 570 Ma continental configurations, respectively.

CPD
9, 3615–3662, 2013

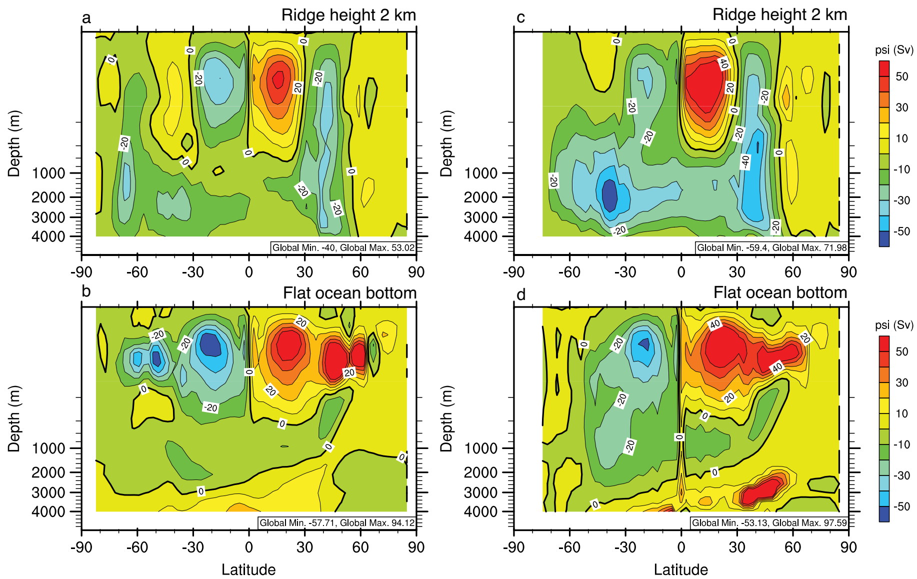

Fig. 6. Similar to Fig. 4 but here the zonally integrated total (Eulerian plus eddy-induced) Meridional overturning circulation (MOC) is shown. Note that the maximum value for the 570 Ma continental configuration (**c** and **d**) is much larger than that for the 720 Ma continental configuration (**a** and **b**) due to eddy-induced circulation (not shown). TSI = $0.94\mathrm{TSI}_0$, $p\mathrm{CO}_2$ = 2000 ppmv for all four simulations.

CPD
9, 3615–3662, 2013

The initiation of Neoproterozoic "snowball" climates in CCSM

Y. Liu et al.

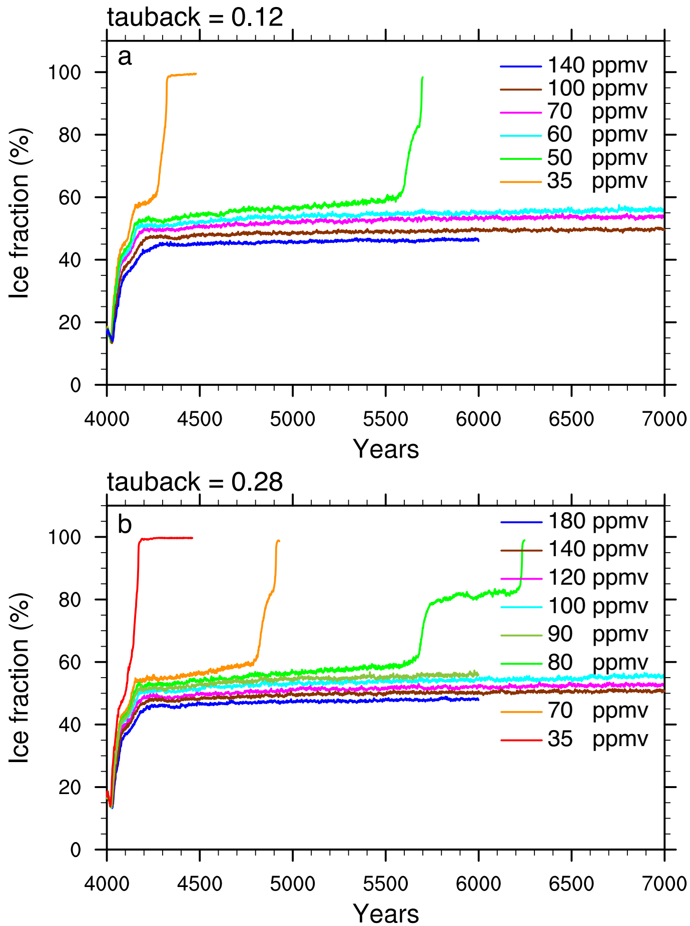

Fig. 7. Time series of sea ice fraction (ratio of total sea ice area to the area of whole ocean) obtained for the branch runs for the 720 Ma continental configuration. The values of tauback are 0.12 in **(a)** and 0.28 in **(b)**. TSI is fixed to be $0.94TSI_0$ for all simulations.

CPD
9, 3615–3662, 2013

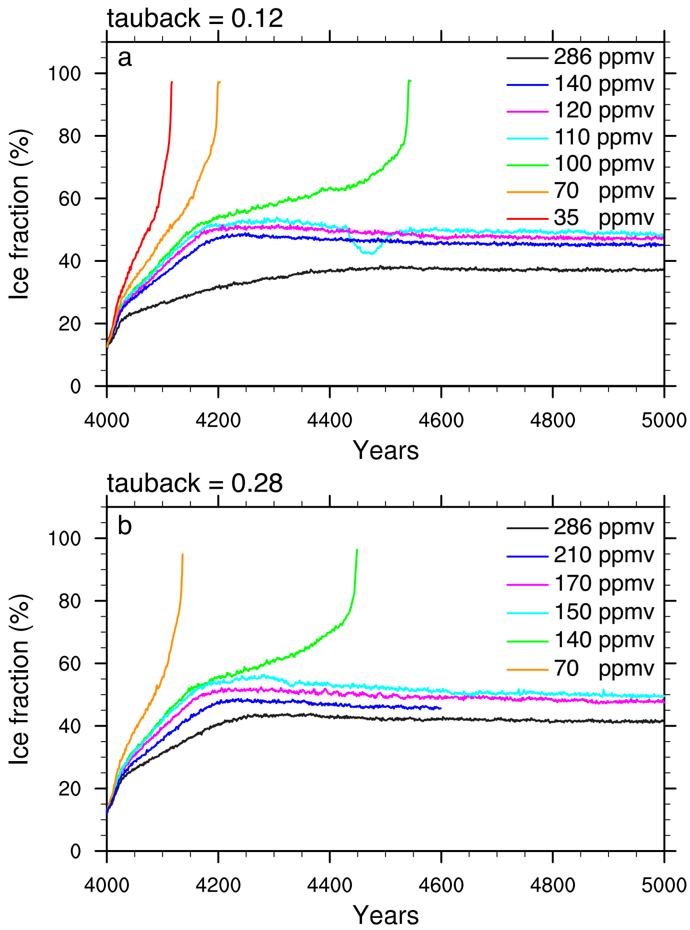

Fig. 8. Same as Fig. 7 except that this is for the 570 Ma continental configuration. TSI is fixed to be $0.94\mathrm{TSI}_0$ for all simulations.

CPD
9, 3615–3662, 2013

The initiation of Neoproterozoic “snowball” climates in CCSM

Y. Liu et al.

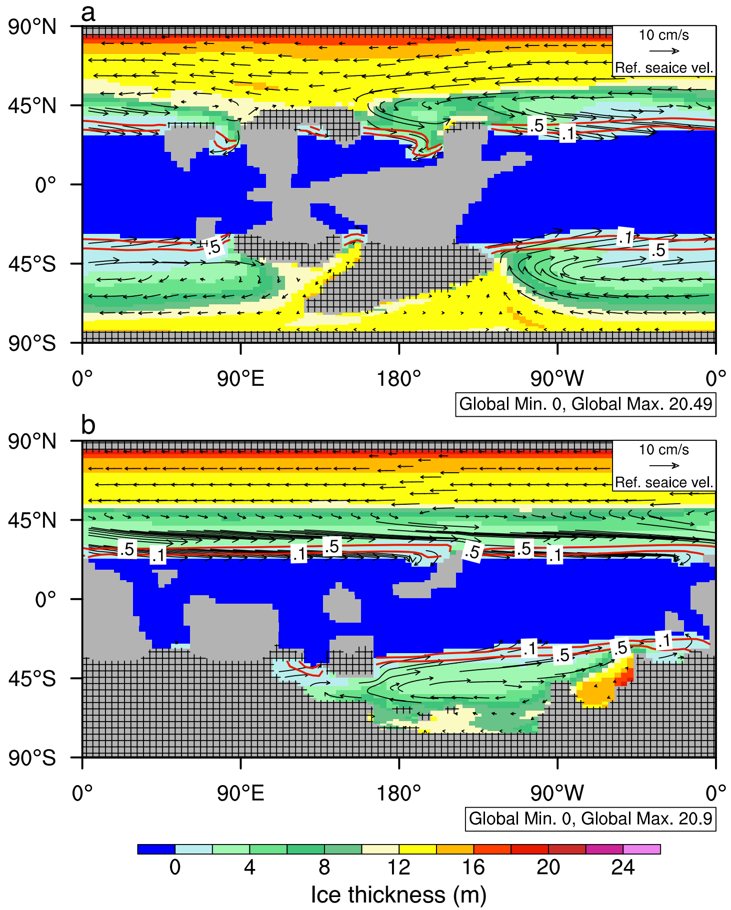

Fig. 9. The same as Fig. 4 except that here pCO_2 = 140 ppmv (TSI is still $0.94TSI_0$) and only the results from DIF method are shown. The results are the average of the last 100 yr of the simulations.

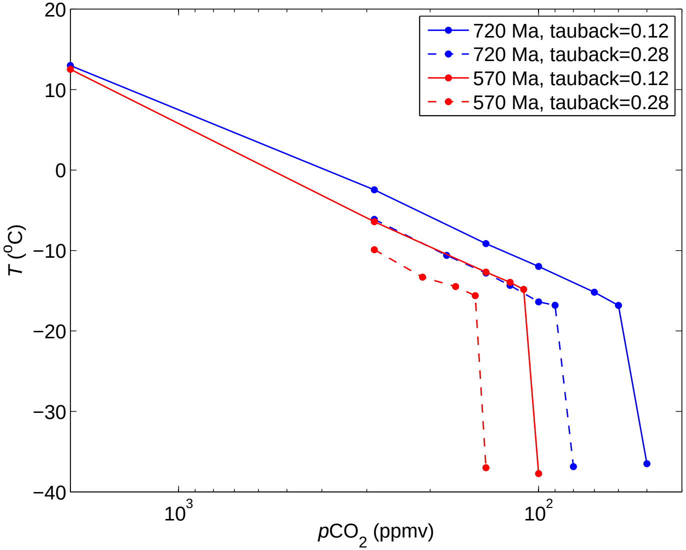

Fig. 10. The change of global mean surface temperature with CO_2. The dots represent the equilibrium state of the runs shown in Figs. 7 and 8. $TSI = 0.94TSI_0$ for all the simulations. The global mean surface temperature obtained for hard snowball state (lowest points of the lines) may be an underestimate because the model either failed or was terminated soon after the climate enters into such a state. Moreover, the sea ice parameterization in the model may not be suitable for that in a hard snowball.

CPD
9, 3615–3662, 2013

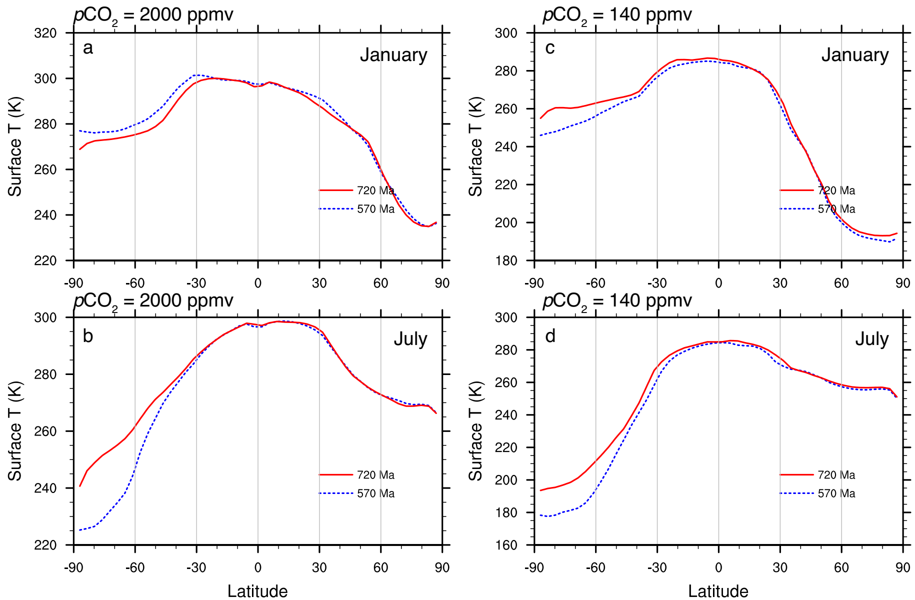

Fig. 11. Zonal mean surface temperature for the control run (**a** and **b**) and branch run (**c** and **d**). TSI = $0.94\mathrm{TSI}_0$ for all the simulations. The upper and lower two panels are for January and July respectively. Similar to Fig. 9, these are also hundred-year mean.

CPD
9, 3615–3662, 2013

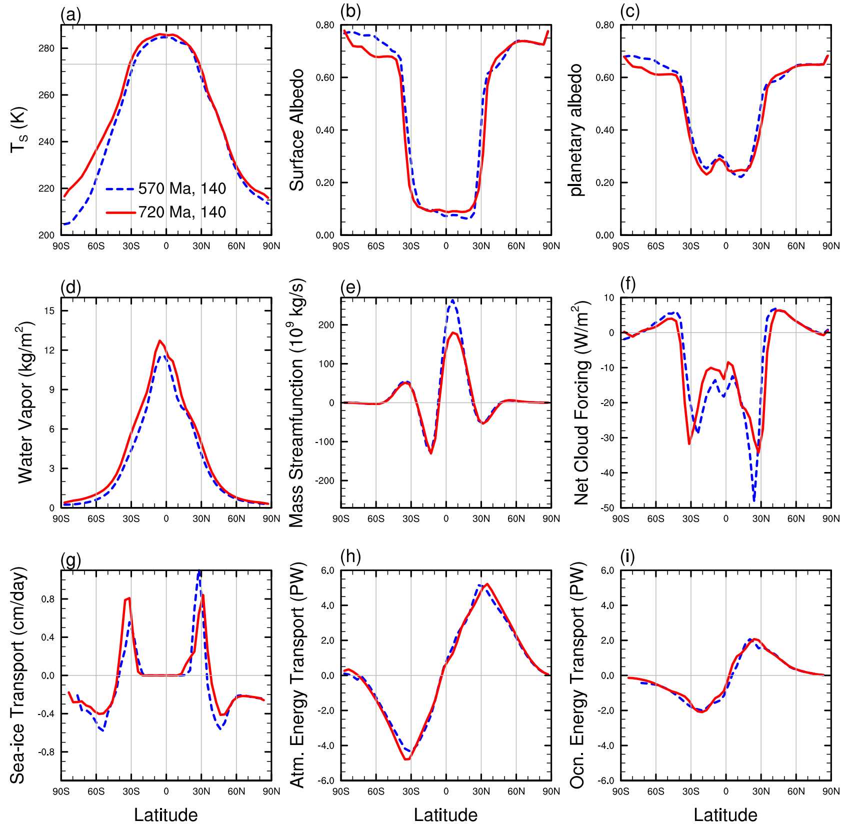

Fig. 12. Comparison of zonal mean surface temperature, surface albedo, planetary albedo, water vapor in the atmospheric column, mass stream function of the atmosphere at 500 milibar, net cloud forcing, sea ice mass change due to sea-ice transport, atmospheric and oceanic heat transport between the two continental configurations. $TSI = 0.94TSI_0$, $pCO_2 = 140$ ppmv and tauback = 0.12 for both runs. The results are from hundred-year average at equilibrium of the simulations.

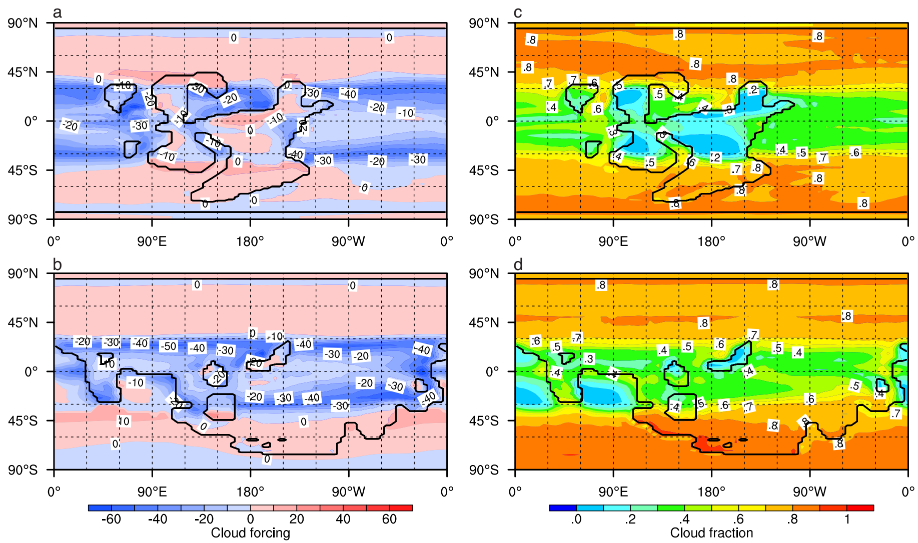

Fig. 13. Similar to Fig. 9 except that here the net cloud forcing (in **a** and **b**) and low-level cloud fraction (in **c** and **d**) are shown. TSI = 0.94TSI_0, pCO_2 = 140 ppmv for both two simulations.

CPD
9, 3615–3662, 2013

The initiation of Neoproterozoic "snowball" climates in CCSM

Y. Liu et al.